ACS APPLIED MATERIALS & INTERFACES

Research Article

www.acsami.org

Sub-10 nm Resistless Nanolithography for Directed Self-Assembly of Block Copolymers

Marta Fernández-Regúlez,[†,∥,⊥] Laura Evangelio,[†,‡,⊥] Matteo Lorenzoni,[†] Jordi Fraxedas,[‡,§] and Francesc Pérez-Murano*[,†]

[†]Instituto de Microelectrónica de Barcelona (IMB-CNM, CSIC), Campus UAB, 08193 Bellaterra, Barcelona, Spain

[‡]Institut Catala de Nanociencia i Nanotecnologia (ICN2), Campus UAB, 08193 Bellaterra, Barcelona, Spain

[§]Consejo Superior de Investigaciones Cientificas (CSIC), Campus UAB, ICN2 Building, 08193 Bellaterra, Barcelona, Spain

Supporting Information

ABSTRACT: The creation of highly efficient guiding patterns for the directed self-assembly of block copolymers by resistless nanolithography using atomic force microscopy (AFM) is demonstrated. It is shown that chemical patterns consisting of arrays of lines defined on a brush layer by AFM allow the alignment of the blocks of lamella-forming polymers. The main advantage of this method relies on the capability to create high-resolution (sub-10 nm line-width) guiding patterns and the reduction of the number of process steps compared to the state-of-the-art methods for creating guiding patterns by chemical surface modification. It is found that the guiding patterns induce the block alignment very efficiently, allowing the achievement of a density multiplication factor of 7 for block copolymers of 14 nm half-pitch, which is attributed to the combined effect of topographical and chemical modification.

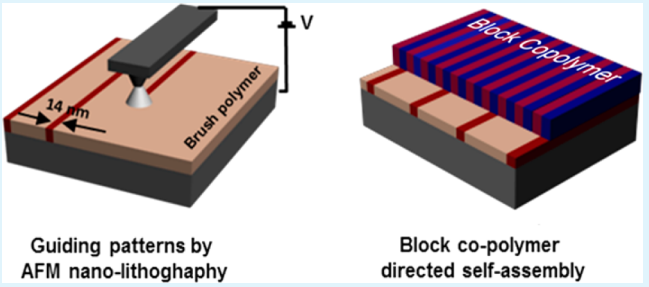

KEYWORDS: *block copolymer self-assembly, atomic force microscopy, chemical guiding patterns*

INTRODUCTION

The miniaturization trend in many areas of science and technology demands the continuous resolution improvement of patterning methods. It occurs in the semiconductor industry, where the increase of density in integrated circuits requires reducing the critical dimensions of transistors, as dictated by Moore's law,[1] and it occurs in other areas such as magnetic storage, energy, or (biochemical) sensing. In all of these fields, convenient patterning methods with resolution below 10 nm is still far from being fully developed. Moreover, when selecting the optimal nanopatterning method, in addition to resolution, other aspects such as throughput, cost, and material/process compatibility come into play.

The most advanced technologies are based on immersion deep ultraviolet (DUV) optical lithography,[2] which allows a high throughput at the expense of extreme complexity and cost. Any alternative to immersion DUV for industrial applications is still under development, such as extreme UV optical lithography or maskless parallel e-beam lithography. For research purposes, electron beam lithography,[3] scanning probe lithography,[4] and focused electron beam and ion beam processing[5] are examples of techniques able to pattern sub-10 nm features at the expenses of low throughput. Additional techniques capable of simultaneously providing high resolution and high throughput are nanoimprint lithography[6,7] and related printing-based techniques, which are especially convenient for patterning of biological entities.[8]

On the other hand, directed self-assembly (DSA) of block copolymers (BCP) allows patterning surfaces at high resolution[9−11] taking advantage of self-organization in confinement.[12] DSA of BCP is becoming a well-established method with a high potential of gaining industrial relevance due to high throughput and process simplification compared to other approaches.[13−15] BCPs are macromolecules that are formed by two (or more) chemically distinct polymer chains (blocks) joined by interblock covalent bonds.[11,16] In order to minimize the contact area between them, the blocks tend to separate due to a balance between repulsive intermolecular and attractive restore forces. This segregation leads to a regular nanometer arrangement of different structural configurations (plates, cylinders, spheres, or other more complex shapes) depending on the ratio of molecular weights of the blocks forming the copolymer.[17] The special interest of the study of these materials lies in the fact that they possess the intrinsic property of forming dense nanoscale structures whose length scales are not accessible using traditional lithographic techniques. Importantly, the DSA of BCP is intended not to replace traditional lithography but to offer and provide a complementary alternative for use; that is, it tries to combine the use of traditional lithographic techniques to create patterns, along

Received: September 25, 2014
Accepted: October 31, 2014
Published: October 31, 2014

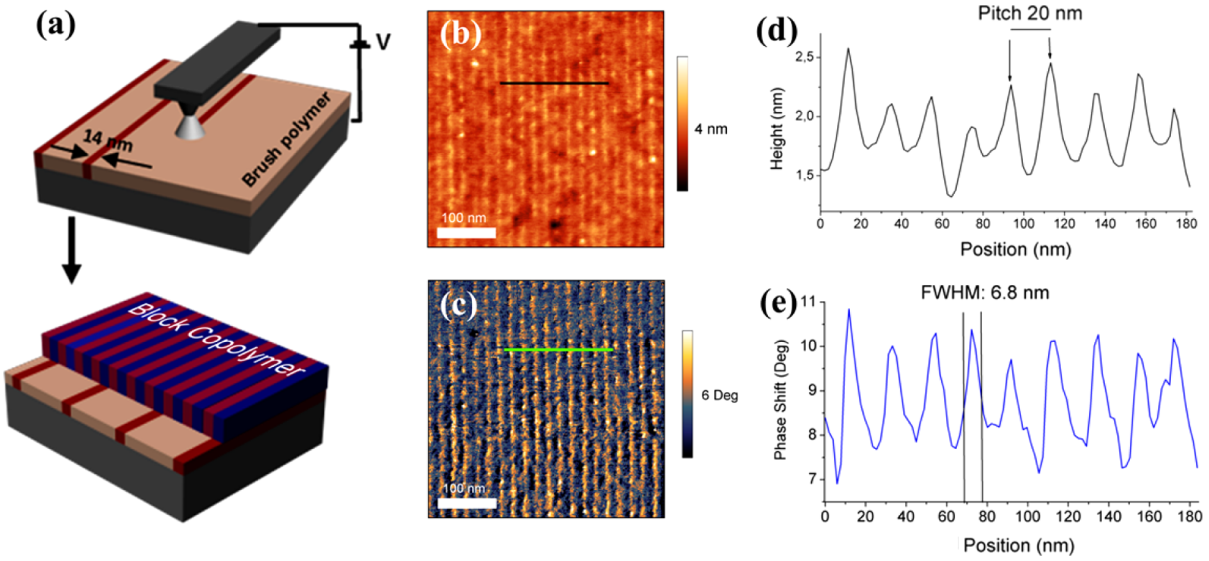

Figure 1. (a) Scheme of the process for DSA of BCP by AFM nanolithography. The AFM tip creates chemical patterns by local anodic oxidation on a PS−OH brush layer. After creation of the guiding pattern, the block copolymer is deposited and annealed. The two phases of the lamella forming block copolymer (PS and PMMA) become oriented in the way dictated by the guiding patterns. (b) Topographic AFM image of an array of lines of 20 nm pitch (Δz = 4 nm). Patterning conditions: bias voltage, 32.5 V; tip speed, 20 μm/s. (c) Phase image acquired simultaneously to image b ($\Delta\Phi$ = 6°). (d) Profile extracted from image b. (e) Profile extracted from image c.

with the engineering of new processes and materials, in order to facilitate cost-effective techniques for the multiplication of pattern density and defect rectification. Many efforts are now being focused toward the development of computational methods for DSA,[18] and recent works have demonstrated three-dimensional nanofabrication by block copolymers.[19]

Highly oriented and ordered patterns can be achieved by conveniently creating guiding patterns on the surface, by either graphoepitaxy[20−23] or chemical epitaxy.[24−26] Graphoepitaxy is based on creating topographic patterns (usually holes or trenches) and confine the BCP on it. Graphoepitaxy is commonly used in combination with cylinder-forming BCPs in order to shrink the size of contact holes or to achieve contact-hole multiplication.

Chemical epitaxy is the method of choice for producing high-density patterns. It consists of creating chemical patterns on a neutral surface so the modified areas of the surface would present larger affinity to one of the blocks, determining the position and orientation of the molecules. Density multiplication is defined as the ratio between the period of the guiding pattern with respect to the period of the directed self-assembled pattern. In consequence, density multiplication allows the decrease of the requirements of the lithography method for creating the guiding pattern in terms of resolution and throughput. Density multiplication factors of 10× has been reported for graphoepitaxy[27] and 9× for chemical epitaxy in the case of cylindrical-forming PS-*b*-PMMA block copolymers.[28]

Chemical guiding patterns are created on neutral surfaces that are usually prepared by depositing or grafting a polymer brush layer, which presents equal affinity for both blocks of the copolymer. The procedure for defining the chemical guiding pattern consists of creating a mask on top of the brush layer and using this mask for a selective etching or exposure process. The mask is created by means of a lithography process that requires high-resolution accuracy, and therefore, either DUV optical lithography or electron beam lithography are commonly used. This as-created mask protects selected areas of the surface, while the rest of the areas are chemically modified either by exposing them to an oxygen plasma[29,30] or by selectively removing the neutral layer and later replacing it with another polymer with different chemical affinity.[31]

DUV lithography is usually the method of choice for defining the guiding pattern,[2] but the availability of DUV equipment is very limited in a research environment, and the required accuracy for the guiding patterns may reach the limit achievable for this technique, which is becoming crucial for block copolymers of small dimensions, as required for the next generation of chips manufacturing.[32] Electron beam lithography is then used for exploration and research purposes,[3,29,31] but then the throughput is much lower, and to obtain resolution below 10 nm requires critical processing conditions[33] or use of specific resists.[34]

Here, we demonstrate the creation of guiding patterns for directing the self-assembly of BCPs by means of atomic force microscopy (AFM) based nanolithography. The resulting procedure has fewer single process steps than DUV- or electron beam lithography (EBL)-based processing, because the pattern is directly created on the neutral layer without the need of spinning a resist and further chemical development. Moreover, the unique capabilities of AFM, in terms of resolution and position accuracy, make its use highly convenient for the investigation of the guiding behavior of novel polymer materials, particularly those that are of very small block size, in view of obtaining a half-pitch resolution around 10 nm or below.

Very few attempts to create guiding patterns by AFM for directing the self-assembling of block copolymer have been reported.[35,36] In those works, a self-assembled layer of octadecyltrichlorosilane (OTS) is chemically modified by contact-mode AFM while applying a voltage and then cylindrical BCPs are assembled. Pattern guiding is used to study the accommodation of polymers to different guiding pattern size. Here, we report the application of the local anodic oxidation AFM method,[37,38] (also referred to oxidation scanning probe lithography, o-SPL[39]) for the creation of guiding patterns for lamella forming BCPs, which induce the

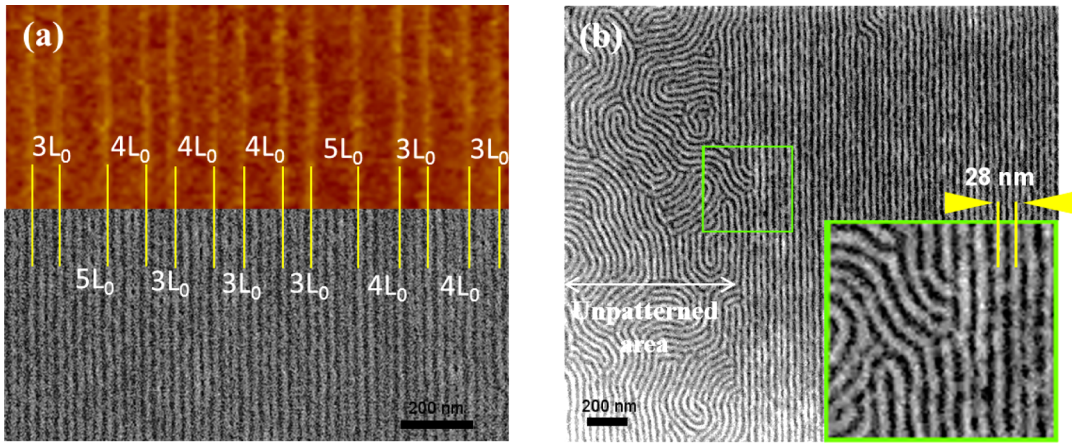

Figure 2. Density multiplication in DSA of PS-*b*-PMMA block copolymers induced by a guiding pattern defined by o-SPL (V = 36 V; tip speed = 3 μm/s; RH = 23%). (a) Comparison between the (top, AFM image) guiding pattern and (bottom) the aligned BCP pattern. SEM images are taken after removing the PMMA block by oxygen plasma etching. Scale bar represents 200 nm. (b) SEM image showing the aligned block copolymer on top of the guiding pattern and the nonaligned polymer on top of the unpatterned area. Scale bar is 200 nm. (Inset) Magnified image of the area indicated by the green square.

formation of aligned arrays of parallel lines with density multiplication factors up to 7. We show that such patterns can be created very efficiently, precisely, and routinely using commercial equipment. o-SPL allows the operation of the AFM in noncontact mode, increasing the tip throughput and lifetime.[37] Because the achievable resolution with o-SPL is below 5 nm,[38] we believe that this approach has great potential to become very useful in the study of BCPs DSA, especially for the next generation of BCPs of low molecular weight.

MATERIALS AND METHODS

Figure 1a shows the overall process for DSA using guiding patterns created by o-SPL on top of brush layers made of hydroxyl-terminated polystyrene (PS−OH). It consists of a three-step process: (1) grafting a brush layer on top of a silicon surface, (2) forming of the guiding patterns by AFM nanolithography, and (3) block copolymer self-assembly. The whole process contains fewer single processes than the usual methods to create chemical guiding patterns, because the sequence of resist, exposure, development, and resist removal is substituted by the single process of o-SPL patterning.

Grafting of the PS−OH Brush Layer. The starting substrates are 0.9 × 0.9 cm chips bearing a native silicon oxide layer (p-type silicon wafers of 4−40 Ω·cm resistivity). The brush layer is created from PS−OH (M_n = 4.5 kg·mol^{-1}, PDI = 1.09), purchased from Polymer Source, Inc. The grafting process starts by coating the silicon surface with the polymer brush. Previously, the silicon surface has been cleaned and activated by O_2 plasma for 10 min to allow the reaction between the hydroxyl groups from the PS−OH and the native oxide of the surface. A 40 nm thick PS−OH brush layer is deposited by spin-coating at 5000 rpm from a 1.5% (w/w) toluene solution. Subsequently, samples are annealed using two different methods: annealing in air or in nitrogen environment. The first one is performed using a preheated hot-plate at 190 °C for 2 min, and the second one is performed in an atmospheric furnace at 260 °C for 5 min with a continuous nitrogen air flow. After the samples are annealed, the unreacted PS−OH is rinsed away with toluene by ultrasonication at 40 °C for 5 min. Brush layers have been characterized by X-ray photoelectron spectroscopy (XPS), and it has been found that the annealing conditions drastically determine the chemical state of the surface (Supporting Information, section S1). When the annealing is performed in an atmospheric environment, the brush layer is damaged and oxidized, while the integrity of the brush polymer layer is preserved when the annealing is performed in a nitrogen environment.

We have checked the neutral character of the brush layer for both blocks of the block copolymer by characterizing the contact angle between the brush layer and PS and PMMA homopolymers, following a procedure described in ref 40. A thin homopolymer layer is deposited on top of a brush layer and then annealed in vacuum environment for 72 h. After that, droplets of the homopolymer are formed on the brush layer, and the contact angle of these droplets is determined by AFM characterization. We have obtained contact angle values of 14° for PS on PS−OH and of 23° for PMMA on PS−OH. Despite the larger affinity to PS−OH, it is good enough to obtain good segregation of phases in vertical lamella form.

Creation of Guiding Patterns By AFM Lithography. Guiding patterns are created on the grafted PS−OH brush layers by o-SPL under noncontact mode operation. The AFM instrument has close-loop correction of X, Y and Z displacement, what facilitates to fabricate patterns of good dimensional quality. Standard noncoated silicon AFM probes have been used (OTESPA, Bruker). The control humidity system works by introducing dry or wet nitrogen air into the AFM chamber to set it in the range 20% - 60% RH. The sequence for creating a guiding pattern is as follow: (1) The AFM is operated in soft tapping mode, at an oscillation amplitude around 15 nm. (2) The AFM tip is moved to the position to start fabricating a line. (3) The feedback-loop is disconnected, and a positive bias voltage is applied to the sample through the AFM chuck. (4) The tip is moved along the line at the selected speed. (5) When the tip reaches the end of the line, the bias voltage is switched to zero, and the feedback loop is connected. (6) The tip is moved to the new position to create the next line. In order to maintain tip−surface separation constant, the lines are fabricated following the direction where the lateral movement of the tip is parallel to the surface.

Block Copolymer Self-Assembly. Poly(styrene-*n*-methyl methacrylate) (PS-*b*-PMMA 50:50, M_n = 35 kg·mol^{-1}, PDI = 1.12), has been used as a block copolymer. The PS-*b*-PMMA powder is dissolved in a 1.15% (w/w) toluene solution. After the o-SPL process, the block copolymer is spin-coated onto the brush layer at 2750 rpm, obtaining a 36 nm film thickness. Afterward, the samples are annealed on a preheated hot-plate at 200 °C for 20 min, in order to self-assemble the block copolymer. Finally, PMMA domains are removed by O_2 plasma (300 W, 10 sccm O_2) for 18 s, in order to characterize the BCP films by SEM.

RESULTS AND DISCUSSION

Because the sequence of resist deposition, exposure, development, selective functionalization, and resist removal is replaced by the single process of o-SPL patterning, the resulting process becomes simpler. The AFM is operated in noncontact mode and it requires the formation of a water meniscus connecting

tip and surface.[41] Under the application of a positive voltage to the sample with respect to the tip, the water meniscus is ionized and OH^- ions are accelerated toward the surface, where the electrochemical reaction takes place. The resolution of the pattern is determined by the AFM tip radius, the size of the water meniscus (which depends on the air humidity), the applied voltage, and the relative velocity of the tip with respect to the surface. Patterns of small line-width are achievable by using high tip-speed (above 10 μm/s) and low ambient humidity. Figure 1b–e shows an example of a high-resolution pattern, consisting on an array of lines of 20 nm pitch with a line width resolution below 10 nm. It is remarkable that the contrast in the phase image (Figure 1c) is larger than in the topographic image (Figure 1b), indicating that the patterning involves changes in the surface chemical properties. The origin of compositional contrast in phase imaging AFM is related to changes in energy dissipation. Consequently, Figure 1c says that in the oxidized regions, the tip dissipates more energy. This is also indicative of differences in the chemical and/or physical properties between the oxidized and unoxidized regions.[42]

The patterns created by o-SPL are highly effective for guiding of BCPs. As AFM can easily produce high resolution patterns, the oxidation conditions are set to obtain a line width similar to the half-length of the BCPs (14 nm), and a pattern pitch equal to an integer multiple of the BCP length.

Figure 2 shows an example of density multiplication obtained by an o-SPL guiding pattern. Figure 2a shows a comparison between the guiding pattern (top, AFM image) and the resulting aligned BCP (bottom, SEM image). The guiding pattern is made of a set of lines of varying pitch in multiples of block copolymer length L_o (28 nm), resulting in density multiplication factors from $3L_o$ to $5L_o$. The frontier between aligned and not aligned areas can be observed in the SEM image of Figure 2b. It demonstrates the effectiveness of the o-SPL for BCP alignment.

Figure 3a shows an array of lines created by o-SPL, covering an area of 15 × 15 μm. A magnified image of the array (Figure 3b) reveals that the patterns consist of lines 15 nm wide and roughly 1 nm high. The fact that the modified areas appear raised from the background indicate oxidation of the underlying substrate, as discussed later. Figure 3d,e shows how the air humidity drastically influences the line resolution. These patterns have been obtained under the same conditions (V = 32.4 V, tip speed = 5 μm/s) except for the ambient humidity, which was raised from 20 to 40%. A closer inspection of the patterns reveals that its roughness is basically dictated by the surface roughness of the brush layer, which is the limiting factor for the present pattern resolution.

Attempts have been made to obtain larger density multiplication factors. We have observed that patterns made of very thin lines, like the one in Figure 1c, are not effective to obtain large density multiplication factors. Increasing the oxidation strength results in a larger guiding effectiveness, even taking into account that the line width of the pattern increases. Figure 4a shows an example of a pattern formed by an array of lines with a separation of 168 nm (6 × 28 nm). The lines that form the pattern are thicker and wider than the ones in Figure 1d. The SEM image of the BCP pattern in Figure 4b shows good alignment after DSA. Remarkably, as the line-width of the guiding line is larger than half of the period of the BCP, density multiplication of 1.5× is also occurring on top of the chemically modified areas, resulting in a total multiplication factor of 7. Figure 4c shows a comparative magnified image of Figure 4a,b.

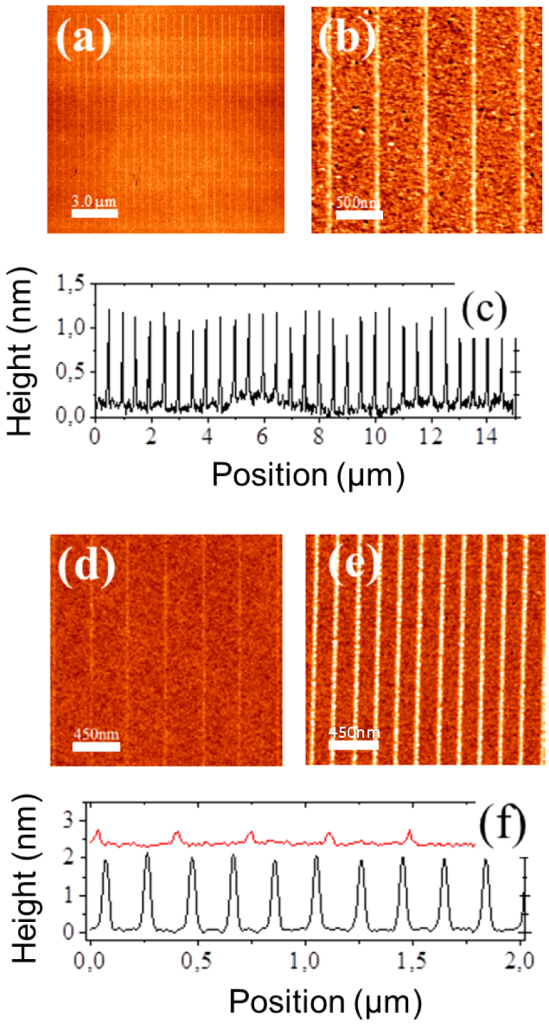

Figure 3. AFM images and profiles of guiding patterns created by o-SPL. (a) Array of lines covering an area of 15 × 15 μm. Patterning conditions: bias voltage, 45 V; tip speed, 1 μm/s; 35% RH. (b) A magnified image of the array reveals that the pattern consists of lines 15 nm wide and roughly 1 nm high. (c) Profile extracted from image a. (d) Array of lines performed at low humidity (20% RH) and (e) at high humidity (40% RH). Both patterns are created under the same conditions (bias voltage, 32.4 V; tip speed, 5 μm/s). (f) Profiles extracted from (red) image d and (black) image e to highlight the effect of relative humidity.

It is observed that the guiding pattern sets the position of the PMMA-block at the center of the guiding pattern, while two polystyrene domains are positioned also on top of the guiding lines. Figure 4d shows a tilted SEM image of a cross-section performed by focused ion beam on the pattern from Figure 4b. The position of the substrate/copolymer interface is depicted by the dashed line, and the two arrows indicate the position of the center of the guiding lines. As the thickness of the oxide is lower than 2 nm, the guiding lines cannot be appreciated in the SEM image.

The guiding patterns formed by o-SPL on the brush layer can be of diverse chemical/physical nature: (1) chemical surface modification of the top groups of the brush layer polymer molecules, similar to what it has been reported on tip-induced electro-oxidation for constructive nanolithography;[43] (2) chemical modification of the brush and oxidation of the underlying silicon; and (3) oxidation of the underlying silicon

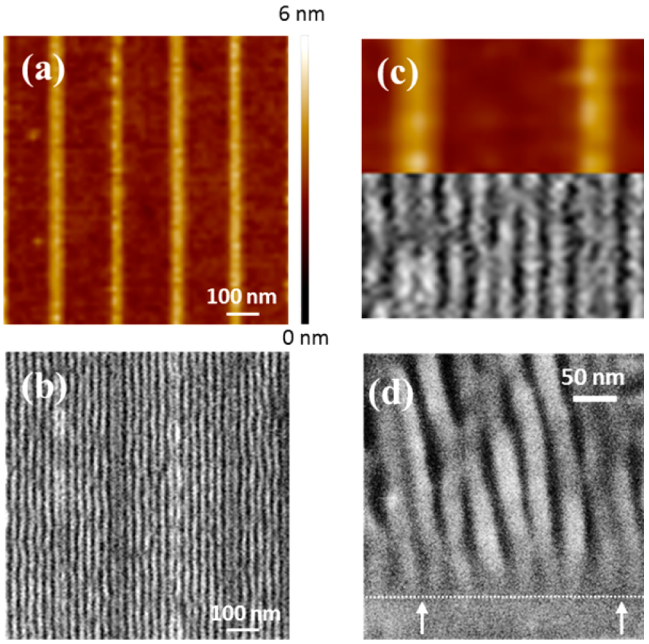

Figure 4. (a) AFM image of a guiding pattern defined by o-SPL (V = 34.2 V; tip speed = 2 μm/s; RH = 38%). (b) SEM image of the BCP-aligned pattern. (c) Comparison between the (top, AFM image) guiding pattern and (bottom) the aligned block copolymer pattern. (d) Tilted SEM image of a cross-section performed on the pattern of image b by focused ion beam, showing the interface between the PS lines of the copolymer and (dashed line) the substrate. The arrows indicate the position of the guiding pattern lines. SEM images are taken after eliminating the PMMA block.

together with degradation of the brush polymer layer. The actual coexistence of these three situations is demonstrated by performing on-purpose experiments.

Situation 1 is identified when the AFM images do not show topographic contrast but show only chemical contrast, as in Figure 1b,c. More experiments on chemical contrast determination are presented in the Supporting Information, section S2. Situations 2 and 3 require that o-SPL oxidation proceeds through the brush layer. Actually, it has been previously reported that the silicon surface can be oxidized through thin polymer layers.[44] The oxidation of the underlying substrate is induced by the transport of OH^- ions through the polymer layer, enhanced by the large electrical field originated from the voltage applied between tip and surface. Discrimination between situations 2 and 3 is achieved by performing patterns at different voltages, followed by a process consisting in immersing the sample in a 5% HF solution for 10 s to remove the silicon oxide (Supporting Information, section S3). The undegraded PS−OH brush layer is resistant to an HF etch, and thus, it protects the silicon oxide to be etched. We have found that, at high voltages, the polymer brush layer degrades.

A close inspection of the aligned BCP patterns (Figure 4) indicates larger affinity of the modified areas to the PS block. This is a different situation than the one reported in the previous example of guiding the alignment of BCPs by AFM,[35,36] in which the terminal methyl groups of an OTS self-assembled monolayer are converted into carboxylic groups, which present higher affinity to the PMMA molecule. A possibility for the nature of the chemical modification in the case of PS−OH brush layers is that the AFM patterning process causes a partial degradation of the PS molecules, increasing its affinity to the PS-block.

The experiments indicate that the simple chemical modification of the brush layer surface alone is not sufficient to guide the alignment, while patterns showing at least 0.5 nm of topographic height contrast efficiently induce the guiding of the BCP. The influence of topography-induced alignment on chemical patterns has been recently studied.[45] This is very relevant for the understanding of the DSA process of future small-size BCP. When employing low-weight (small-length) polymers to obtain DSA patterns of higher resolution, the future requirements for guiding patterns are going to be more stringent. In this context, the unique capabilities of AFM to create patterns of resolution below 10 nm that, in addition, combine topographic and chemical contrast will provide further possibilities for expanding the present limitations of DSA to smaller feature sizes. Moreover, this method can be extended to other polymer material combinations, facilitating the investigation of their self-assembly behavior.

Defectivity is one of the most critical issues for the future industrial applications of DSA. The study of the defectivity and pattern commensurability of the guiding patterns is now under intensive investigation, either in graphoepitaxy[46] or in chemical epitaxy.[47] We have not investigated in detail the defectivity of DSA patterns created by o-SPL, as it would require the creation of numerous large patterns, which will represent a large effort with the present SPL instrumentation.

CONCLUSIONS

In summary, we have presented a method to create guiding patterns for block copolymer DSA by AFM-based nanolithography. The method relies on the unique resolution performance of AFM, and it presents the additional advantage of simplifying the processing sequence by reducing the number of single processing steps. We have shown that the alignment capabilities of the patterns created by AFM are caused by a combination of chemical and topographic contrasts, allowing density multiplication factors up to 7.

The major drawback of AFM nanolithography is the low throughput arising from the limited scan size and speed, which, at present, limits its industrial applicability. However, diverse actions are taken in order to improve it, such as parallelization of AFM lithography by the use of multiple probes[48] or the use of local oxidation with high-resolution stamps.[49,50] In addition, we believe that the approach that we have pursued in this work, based on AFM local anodic oxidation, can be further adapted to other AFM nanolithography methods; for example, it can be used in combination of thermomechanical writing[4] or current-induced exposure of resist at low voltage.[51] In any case, the creation of guiding patterns by o-SPL is a simple and affordable method to study the alignment behavior of BCPs. In this sense, we think that the results that we have presented here will help to get access to more research groups to the experimental investigation on the DSA of BCPs.

ASSOCIATED CONTENT

Supporting Information

Characterization of the PS−OH brush layer; determination of the chemical contrast of the guiding pattern by AFM; characterization of the resistance to HF etching of the PS−OH brush layer modified by o-SPL. This material is available free of charge via the Internet at http://pubs.acs.org.

AUTHOR INFORMATION

Corresponding Author

*E-mail: Francesc.Perez@csic.es.

Present Address

[‖]CEA-LETI, MINATEC Campus, 17 rue des Martyrs, 38054 Grenoble cedex 9, France

Author Contributions

[⊥]The manuscript was written through contributions of all authors. All authors have given approval to the final version of the manuscript. These authors contributed equally.

Funding

This work was partially funded by the projects SNM (FP7-ICT-2011−8), FORCE-for-FUTURE (CSD2010−00024), SiNSoC (MAT2011−15159-E) and NaNeau (MAT2012−38319-C02−01).

Notes

The authors declare no competing financial interest.

ACKNOWLEDGMENTS

We acknowledge previous experiments and technical advice from Lorea Oria and Guillaume Sauthier for technical help in the XPS experiments.

REFERENCES

(1) Moore, G. E. Cramming More Components onto Integrated Circuits. *Electronics* **1965**, *38*, 114−117.

(2) Tiron, R.; Chevalier, X.; Couderc, C.; Pradelles, J.; Bustos, J.; Pain, L.; Navarro, C.; Magnet, S.; Fleury, G.; Hadziioannou, G. Optimization of Block Copolymer Self-Assembly through Graphoepitaxy: A Defectivity Study. *J. Vac. Sci. Technol., B* **2011**, *29*, 1−8.

(3) Ruiz, R.; Kang, H.; Detcheverry, F.; Dobisz, E.; Kercher, D.; Albrecht, T. Density Multiplication and Improved Lithography by Directed Block Copolymer Assembly. *Science* **2008**, *321*, 936−939.

(4) Pires, D.; Hedrick, J. L.; De Silva, A.; Frommer, J.; Gotsmann, B.; Wolf, H.; Knoll, A. W. Nanoscale Three-Dimensional Patterning of Molecular Resists by Scanning Probes. *Science* **2010**, *328*, 732−735.

(5) Utke, I.; Hoffmann, P.; Melngailis, J. Gas-Assisted Focused Electron Beam and Ion Beam Processing and Fabrication. *J. Vac. Sci. Technol., B* **2008**, *26*, 1197−1276.

(6) Chou, S. Y.; Krauss, P. R.; Renstrom, P. J. Imprint Lithography with 25-Nanometer Resolution. *Science* **1996**, *5*, 85−87.

(7) Schift, H. Nanoimprint Lithography: An Old Story in Modern Times? A Review. *J. Vac. Sci. Technol., B* **2012**, *26*, 458−480.

(8) Cavallini, M.; Gentili, D.; Greco, P.; Valle, F.; Bicarini, F. Micro- and Nanopatterning by Lithographically Controlled Wetting. *Nat. Protoc.* **2012**, *7*, 1668−1676.

(9) Park, C.; Yoon, J.; Thomas, E. L. Enabling Nanotechnology with Self Assembled Block Copolymer Patterns. *Polymer* **2003**, *44*, 6725−6760.

(10) Darling, S. B. Directing the Self-Assembly of Block Copolymers. *Prog. Polym. Sci.* **2007**, *32*, 1152−1204.

(11) Farrell, R.; Fitzgerald, T.; Borah, D.; Holmes, J.; Morris, M. Chemical Interactions and Their Role in the Microphase Separation of Block Copolmer Thin Films. *Int. J. Mol. Sci.* **2009**, *10*, 3671−3712.

(12) Gentili, D.; Valle, F.; Albonetti, C.; Liscio, F.; Cavallini, M. Self-Organization of Functional Materials in Confinement. *Acc. Chem. Res.* **2014**, *48*, 2692−2699.

(13) Rahsack, B.; Somervell, M.; Muramatsu, M.; Tanouchi, K.; Kitano, T.; Nishimura, E.; Yatsuda, K.; Nafus, K. Advances in Directed Self Assembly Integration and Manufacturability at 300 mm. *Proc. SPIE* **2013**, 8682.

(14) Liu, C. C.; Thode, C. J.; Delgadillo, P. A.; Craig, G. S.; Nealey, P. F.; Gronheid, R. Keeping Up with Moore's Law Using Directed Self-Assembly (DSA). *J. Vac. Sci. Technol., B* **2011**, *29*, 06F203.

(15) Liu, G.; Thomas, C. S.; Craig, G. S.; Nealey, P. F. Integration of Density Multiplication in the Formation of Device-Oriented Structures by Directed Assembly of Block Copolymer−Homopolymer Blends. *Adv. Funct. Mater.* **2010**, *20*, 1251−1257.

(16) Fasolka, M.; Mayes, A. M. Block Copolymer Thin Films: Physics and Applications. *Annu. Rev. Mater. Res.* **2001**, *31*, 323−355.

(17) Bates, F.; Fredrickson, G. Block Copolymer Thermodynamics: Theory and Experiment. *Annu. Rev. Phys. Chem.* **1990**, *41*, 525−557.

(18) Fühner, T.; Welling, U.; Müller, M.; Erdmann, A. Rigorous Simulation and Optimization of the Lithography/Directed Self-Assembly Co-Process. *Proc. SPIE* **2014**, 90521C.

(19) Ross, C. A.; Berggren, K. K.; Cheng, J. Y.; Jung, Y. S.; Chang, J. B. Three-Dimensional Nanofabrication by Block Copolymer Self-Assembly. *Adv. Mater.* **2014**, *26*, 4386−4396.

(20) Segaleman, R. A.; Yokoyama, H.; Kramer, E. J. Graphoepitaxy of Spherical Domain Block Copolymer Thin Films. *Adv. Mater.* **2001**, *13*, 1152−1155.

(21) Cheng, J. Y.; Ross, C. A.; Thomas, E. L.; Smith, H. I.; Vancso, G. J. Fabrication of Nanoestructures with Nanostructures with Long-Range Order Using Block Copolymer Lithography. *Appl. Phys. Lett.* **2002**, *81*, 3657−3659.

(22) Park, S.; Lee, D. H.; Xu, J.; Kim, B.; Hong, S. W.; Jeong, Y.; Xu, T.; Russell, T. P. Macroscopic 10-Terabit-Per-Square Inch Arrays from Block Copolymers with Lateral Order. *Science* **2009**, *323*, 1030−1033.

(23) Tiron, R.; Chevalier, X.; Gaugiran, S.; Pradelles, J.; Fontaine, H.; Couderc, C.; Pain, L.; Navarro, C.; Chevolleau, T.; Cunge, G.; Delalande, M.; Fleury, G.; Hadziioannou, G. Pattern Density Multiplication by Direct Self Assembly of Block Copolymers: Toward 300 mm CMOS Requirements. *Proc. SPIE* **2012**, *8323*, 83230O.

(24) Tada, Y.; Akasaka, S.; Yoshida, H.; Hasegawa, H.; Dobisz, E.; Kercher, D.; Takenaka, M. Directed Self-Assembly of Diblock Copolymer Thin Films on Chemically-Patterned Substrates for Defect-Free Nano-Patterning. *Macromolecules* **2008**, *41*, 9267−9276.

(25) Kim, S. O.; Solak, H. H.; Stoykovich, M. P.; Ferrier, N. J.; de Pablo, J. J.; Nealey, P. F. Epitaxial Self-Assembly of Block Copolymers on Lithographically Defined Nanopatterned Substrates. *Nature* **2003**, *424*, 411−414.

(26) Edwards, E. W.; Stoykovic, M. P.; Solak, H. H.; Nealey, P. F. Long-Range Order and Orientation of Cylinder-Forming Block Copolymers on Chemically Nanopatterned Striped Surfaces. *Macromolecules* **2006**, *39*, 3598−3607.

(27) Jeong, S. J.; Moon, H. S.; Kim, B. H.; Kim, J. Y.; Yu, J.; Lee, S.; Lee, M. G.; Choi, H. Y.; Kim, S. O. Ultralarge-Area Block Copolymer Lithography Enabled by Disposable Photoresist Prepatterning. *ACS Nano* **2010**, *4*, 5181−5186.

(28) Tada, Y.; Akasaka, S.; Takenaka, M.; Yoshida, H.; Ruiz, R.; Dobisz, E.; Hasegawa, H. Nine-Fold Density Multiplication of hcp Lattice Pattern by Directed Self-Assembly of Block Copolymer. *Polymer* **2009**, *50*, 4250−4256.

(29) Detcheverry, F. A.; Liu, G.; Neale, P. F.; de Pablo, J. J. Interpolation in the Directed Assembly of Block Copolymers on Nanopatterned Substrates: Simulation and Experiments. *Macromolecules* **2010**, *43*, 3446−3454.

(30) Oria, L.; de Luzuriaga, A. R.; Alduncin, J.; Perez-Murano, F. Polystyrene As a Brush Layer for Directed Self-Assembly of Block Co-Polymers. *Microelectron. Eng.* **2013**, *110*, 234−240.

(31) Liu, C. C.; Han, E.; Onses, M. S.; Thode, C. J.; Ji, S.; Gopalan, P.; Nealey, P. F. Fabrication of Lithographically Defined Chemically Patterned Polymer Brushes and Mats. *Macromolecules* **2011**, *44*, 1876−1885.

(32) Sanders, D. P. Advances in Patterning Materials for 193 nm Immersion Lithography. *Chem. Rev.* **2010**, *110*, 321−360.

(33) Yasin, S.; Hasko, D. G.; Ahmed, H. Fabrication of 5 nm Width Lines in Poly(methylmethacrylate) Resist Using a Water:Isopropyl Alcohol Developer and Ultrasonically-Assisted Development. *Appl. Phys. Lett.* **2001**, *78*, 2760−2762.

(34) Grigorescu, A. E.; van der Krogt, M. C.; Hagen, C. W.; Kruit, P. 10 nm Lines and Spaces Written in HSQ Using Electron Beam Lithography. *Microelectron. Eng.* **2007**, 822−824.

(35) Xu, J.; Park, S.; Wang, S. L.; Russell, T. P.; Ocko, B. M.; Checco, A. Directed Self-Assembly of Block Copolymers on Two-Dimensional Chemical Patterns Fabricated by Electro-Oxidation Nano Lithography. *Adv. Mater.* **2010**, *22*, 2268−2272.
(36) Xu, J.; Russell, T. P.; Ocko, B. M.; Checco, A. Block Copolymer Self-Assembly in Chemically Patterned Squares. *Soft Matter* **2011**, *7*, 3915−3919.
(37) Pérez-Murano, F.; Abadal, G.; Barniol, N.; Servat, J.; Gorostiza, P.; Sanz, F. Nanometer-Scale Oxidation of Si (100) Surfaces by Tapping Mode Atomic Force Microscopy. *J. Appl. Phys.* **1995**, *78*, 6797−6801.
(38) Martinez, R. V.; Losilla, N. S.; Martinez, J.; huttel, Y.; Garcia, R. Patterning Polymeric Structures with 2 nm Resolution at 3 nm Half Pitch in Ambient Conditions. *Nano Lett.* **2007**, *7*, 1846−1850.
(39) Garcia, R.; Knoll, A. W.; Riedo, E. Advanced Scanning Probe Lithography. *Nat. Nanotechnol.* **2014**, *9*, 577−587.
(40) Bokyung, K.; Ryu, D. Y. Dewetting of PMMA on PS-Brush Substrates. *Macromolecules* **2009**, *42*, 7919−7923.
(41) García, R.; Calleja, M.; Pérez-Murano, F. Local Oxidation of Silicon Surfaces by Dynamic Force Microscopy: Nanofabrication and Water Bridge Formation. *Appl. Phys. Lett. 72*, 2295−2297.
(42) Garcia, R.; Magerle, R.; P, R. Nanoscale Compositional Mapping with Gentle Forces. *Nat. Mater.* **2007**, *6*, 405−411.
(43) Maoz, R.; Frydman, E.; Cohen, S. R.; Sagiv, J. Constructive Nanolithography: Inert Monolayers as Patternable Templates for In-Situ Nanofabrication of Metal-Semiconductor-Organic Surface Structures—A Generic Approach. *Adv. Mater.* **2000**, *12*, 725−731.
(44) Martín, C.; Rius, G.; Borrisé, X.; Pérez-Murano, F. Nanolithography on Thin Layers of PMMA Using Atomic Force Microscopy. *Nanotechnology* **2005**, *16* (8), 1016−1022.
(45) Kodera, K.; Sato, H.; Kanai, H.; Seino, Y.; Kihara, N.; Kasahara, Y.; Kobayashi, K.; Miyagi, K.; Minegishi, S.; Yatsuda, K.; Fujiwara, T.; Hirayanagi, N.; Kawamonzen, Y.; Azuma, T. Defect-Aware Process Margin for Chemo-Epitaxial Directed Self-Assembly Lithography Using Simulation Method Based on Self-Consistent Field Theory. *Proc. SPIE* **2014**, 904926.
(46) Keen, I.; Cheng, H. H.; Yu, A.; Jack, K. S.; Younkin, T. R.; Leeson, M. J.; Whittaker, A. K.; Blakey, I. Behavior of Lamellar Forming Block Copolymers under Nanoconfinement: Implications for Topography Directed Self-Assembly of Sub-10 nm Structures. *Macromolecules* **2013**, *47*, 276−283.
(47) Khaira, G. S.; Qin, J.; Garner, G. P.; Xiong, S.; Wan, L.; Ruiz, R.; Jaeger, H. M.; Nealey, P. F.; de Pablo, J. J. Evolutionary Optimization of Directed Self-Assembly of Triblock Copolymers on Chemically Patterned Substrates. *ACS Macro Lett.* **2014**, *3*, 747−775.
(48) Vettiger, P.; Cross, G.; Despont, M.; Drechsler, U.; Durig, U.; Gotsmann, B.; Haberle, W.; Lantz, M. A.; Rothuizen, H. E.; Binnig, G. K. the "Millipede"-Nanotechnology Entering Data Storage. *IEEE Trans. Nanotechnol.* **2002**, *1*, 39−55.
(49) Cavallini, M.; Mei, P.; Biscarini, F.; García, R. Parallel Writing by Local Oxidation Nanolithography with Submicrometer Resolution. *Appl. Phys. Lett.* **2003**, *83*, 5286−5288.
(50) Albonetti, C.; Martinez, J.; Losilla, N. S.; Greco, P.; Cavallini, M.; Borgatti, F.; Montecchi, M.; Pasquali, L.; Garcia, R.; Biscarini, F. Parallel-Local Anodic Oxidation of Silicon Surfaces by Soft Stamps. *Nanotechnology* **2008**, *19*, 435303.
(51) Neuber, C.; Ringk, A.; Kolb, T.; Wieberger, F.; Strohriegl, P.; Schmidt, H. W.; Fokkema, V.; Cooke, M.; Rawlings, C.; Dürig, U.; Knoll, A. W.; de Marneffe, J. F.; de Schepper, P.; Kaestner, M.; Krivoshapkina, Y.; Budden, M.; Rangelow, I. W. Molecular Glass Resists for Scanning Probe Lithography. *Proc. SPIE* **2014**, 90491V.